

Subbarrier photofission of ^{238}U

B. S. Bhandari

DPh-N/MF, CEN Saclay, BP 2, 91190 Gif-sur-Yvette, France

(Received 24 March 1980)

Subbarrier photofission cross sections and the fission half-lives have been calculated for ^{238}U in terms of a suitable double-hump fission barrier model. The competition due to the gamma deexcitation to the shape isomeric state in the second well (and its consequent fission) has been included by introducing an absorptive part in the potential in the second well region. The calculated cross sections reproduce satisfactorily the recently observed "shelf" in the deep-subbarrier energy region and result in a resonance structure in the threshold region consistent with that observed. The calculation also predicts several low energy resonances in the cross sections and a detailed competition of the prompt and the delayed fission contributions suggests that an angular anisotropy measurement might be more sensitive in detecting the relatively small contribution of delayed fission in the energy region 4.5–5.5 MeV.

NUCLEAR REACTIONS Fission calculated subbarrier photofission cross sections and fission half lives using a suitable two-hump fission barrier in ^{238}U . The results reproduce the observed "shelf" in the cross sections in the deep-subbarrier energy region and the observed resonance structure in threshold region.

I. INTRODUCTION

During the last decade we have witnessed a great revival of interest in the study of the physics of nuclear fission. This has been due to parallel developments in experiments and theory during this period and has brought about a significant improvement in our understanding of the process. By adding single-particle effects (shell corrections) to the collective (i.e., liquid-drop) component of the nuclear potential energy, Strutinsky¹ first introduced the concept of a double-humped fission barrier in the actinide nuclei. This so-called "Strutinsky prescription" has since been extended by several other authors in multidimensional calculations of the nuclear potential energy and has resulted in predicting two- and three-humped fission barriers in various actinide nuclei. As the typical heights of these fission barriers are around 5–6 MeV, it is necessary to study the energy dependence of the fission cross sections and of the fission-fragment angular distributions at low excitations in order to determine the details of the fission barrier shapes which seem to be responsible for several interesting subbarrier fission phenomena such as broad and narrow intermediate structures in fission cross sections, the existence of the fission isomers, and the recently discovered "isomeric shelf" in the deep-subbarrier photofission cross sections. At such low excitations, the fission process is supposed to proceed entirely via barrier penetration and the energy dependence of the fission cross sections in

this energy region should therefore reflect the shape of the fission barrier.

The measurements most suitable for such investigations are the low energy neutron-induced fission, the direct-reaction-induced fission, and the photofission or electrofission processes. Although it is now possible to study various particle-induced fission processes with a much higher energy resolution of the order of a few keV,² the excitation spectra of the fissioning nuclei in these reactions are rather complex due to a large variety of spin and angular momenta introduced by the exciting particle. Furthermore, most of these measurements have as yet been restricted to energies very close to the top of the fission barriers, thus providing information only about the barrier shapes at such high excitations. This limitation is due to the fact that neutron-induced fission obviously cannot be used below the neutron binding energies which are also of the order of 5–6 MeV in the actinide nuclei and due mainly to the difficulties associated with a relatively large background in direct-reaction-induced fission cross sections below 10^{-4} – 10^{-5} b. In order to study the details of the barrier shapes at excitations well below the top of the barriers, the photofission and electrofission processes are therefore an excellent means especially because of the restricted angular momenta in the entrance channel corresponding mainly to the dipole and the quadrupole photoabsorption leading to 1^- and 2^+ transition states, respectively, in the fission of even-even nuclei. This particular feature of the

limited angular momenta in photofission processes was pointed out by Bohr³ long before the realization of two- and three-humped fission barriers in actinide nuclei. The importance of the photofission process in investigating the details of such multi-hump fission barriers at low excitations in the actinide nuclei has since been emphasized in recent review papers by Huizenga⁴ and by Bhandari and Nascimento.⁵

Unfortunately the relative weakness of the electromagnetic interaction results in very low cross sections in photofission and electrofission processes, thus rendering such measurements extremely difficult as well as very time consuming. In view of the extremely low cross sections in the subbarrier energy region ranging from approximately 10^{-11} b near 3 MeV of photon energy to the order of a few mb at 6 MeV of photon energy, it becomes essential to use very intense gamma flux in these measurements. Such intense gamma-flux is currently available only through the electron bremsstrahlung beams either from low energy, high current microtrons or from electron linear accelerators with similar characteristics. The use of bremsstrahlung beams in such investigations introduces the usual problems connected with the unfolding of the measured yield curves obtained with a continuous gamma-ray spectrum and results in a relatively poor energy resolution. However, by using the experimentally measured form of the bremsstrahlung spectrum and because of the fact that the fission cross section changes very rapidly (exponentially) in the subbarrier energy region, such difficulties with unfolding procedures are to some extent circumvented. Despite these serious limitations, it is truly remarkable that subbarrier photofission cross-section measurements have recently been extended to very low photon energies of the order of 3 MeV where cross sections of the order of 10^{-11} – 10^{-10} b have been measured.⁶⁻¹²

In Sec. II we compare photofission cross sections of the even-even nucleus ^{238}U near fission threshold revealing resonance structure obtained in various measurements using different photon sources, discuss qualitatively the occurrence of the isomeric shelf in deep-subbarrier photofission cross sections, and define the purpose of the present work devoted to the calculation of such cross sections. Sections III and IV deal with the calculation of the fission penetrability and that of the photofission cross sections, respectively, within the framework of a double-humped fission barrier model. In Sec. V we compare the results of our calculation of cross sections and of fission half-lives with those measured and discuss these with particular emphasis on the shape of the double-humped fission barrier in ^{238}U .

II. STATUS OF EXPERIMENTAL RESULTS AND PURPOSE OF PRESENT WORK

A. Status of experimental results

1. Threshold photofission

Subbarrier photofission cross section measurements have recently succeeded in revealing the presence of resonance structure in fission cross sections at energies close to the top of the barriers. The typical results of such measurements using different photon sources in ^{238}U are summarized in Fig. 1. In this figure the solid line represents the results of Rabotnov *et al.*¹³ using bremsstrahlung; this is a gross resolution measurement and suffers typically from poor knowledge of the bremsstrahlung spectrum needed in unfolding the cross sections from the measured fission yields. The open circles represent the results of Mafra *et al.*¹⁴ using discrete neutron-capture γ rays. These γ rays are extremely narrow with widths of the order of a few electron volts. One therefore has to exercise caution in identifying this structure with that of the previous experiment because, with this technique, one could be sensitive to the structure in the entrance channel corresponding to excitation of individual compound nuclear states. The dashed and dash-dot curves represent respectively the results of Khan and Knowles¹⁵ and those of Anderl *et al.*¹⁶ using Compton scattered capture gamma rays, a method which has an energy resolution intermediate between the

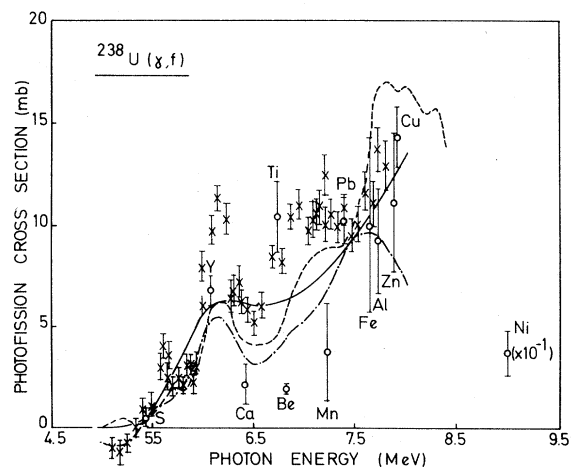


FIG. 1. Measurements of threshold photofission cross sections in ^{238}U . The solid line represents the results of Rabotnov *et al.* (Ref. 13), the dashed curve is the result of Khan and Knowles (Ref. 15), and the dash-dot curve is from Anderl *et al.* (Ref. 16). The crosses represent the results of Dickey and Axel (Ref. 17). Open circles are the points from Mafra *et al.* (Ref. 14) using gamma rays from neutron capture on various elements as labeled in the diagram.

methods previously mentioned. Measurements¹⁵ with this technique exhibit evidence of resonance structure in photofission cross sections of ^{238}U at 5.2, 5.7, 6.2, 7.1, and 7.8 MeV. The crosses are the results of Dickey and Axel¹⁷ using "tagged" bremsstrahlung, a method claiming better resolution than Compton scattered neutron-capture gamma rays. These results appear to confirm the resonances of Ref. 15 except at the lowest energy (5.2 MeV). The cross section, however, is significantly larger.

Monoenergetic photon beams have also been produced recently by in-flight annihilation of monoenergetic positrons at Saclay¹⁸ and at Livermore¹⁹ and have been used in an extensive series of measurements of actinide nuclei by a joint Los Alamos/Livermore collaboration. These measurements have also resulted in cross sections similar to those shown in Fig. 1 and a comparison of these results with some of those shown in Fig. 1 can be seen in Ref. 19. The use of such monoenergetic photons is limited, however, to energies either very close to or above the fission threshold because of a relatively low gamma flux, thus necessitating extremely long exposure times in sub-barrier photofission measurements. Such measurements using bremsstrahlung beams with improved energy resolution using high current microtrons have also been reported more recently^{20,21} with similar results.

2. Isomeric shelf

More recent deep-subbarrier photofission measurements⁶⁻¹² have confirmed the predicted²² presence of an isomeric shelf in this energy region in several actinide nuclei. The presence of such a "shelf" in the cross sections (Fig. 5), meaning an abrupt decrease in the slope, is attributed to the delayed fission on the assumption²² that at these energies gamma deexcitation to the fission isomer (ground state in the second minimum of a double-humped barrier) is competitive with direct decay by fission from the second well. Since there is no time selection of the fission events in these photofission measurements the observed cross sections, representing the sum of the prompt and the delayed fission, exhibit a relatively slowly varying and dominant contribution of the delayed fission in the form of a shelf in the energy region 2.5–4.5 MeV. The fission fragment angular distribution on the shelf is expected²² and has indeed been found²³ to be isotropic since a gamma-ray cascade, which destroys the reference to the incoming photon beam, takes place before the isomer undergoes fission. When the incident photon energy falls below the isomer excitation

energy, the cross section begins to drop again much more rapidly as shown in Figs. 3 and 5.

B. Purpose of present work

The purpose of this paper is to calculate the subbarrier photofission cross sections of ^{238}U in the framework of a two-hump fission barrier model. We have attempted in this work to determine a single suitable set of double-humped barrier parameters for ^{238}U which reproduces satisfactorily the observed resonance structure in the cross section near fission threshold as well as the observed isomeric shelf in the deep-subbarrier photofission cross sections. In addition, the obtained set of barrier parameters is also consistent with the observed isomeric excitation energy, the isomeric half-life, and the ground state spontaneous fission half-life of this nucleus. It is our hope that such a simultaneous analysis of a number of observed fission characteristics in terms of a single set of barrier parameters should prove useful in determining the adequacy of a one-dimensional description of the potential shapes using a set of smoothly joined parabolic potentials to parametrize a double-humped fission barrier.

III. FISSION PENETRABILITY CALCULATION

A. Formalism

The penetrability through a double-humped fission barrier in ^{238}U has been calculated in the WKB approximation. The potential barrier (Fig. 2) has been parametrized by smoothly joining three

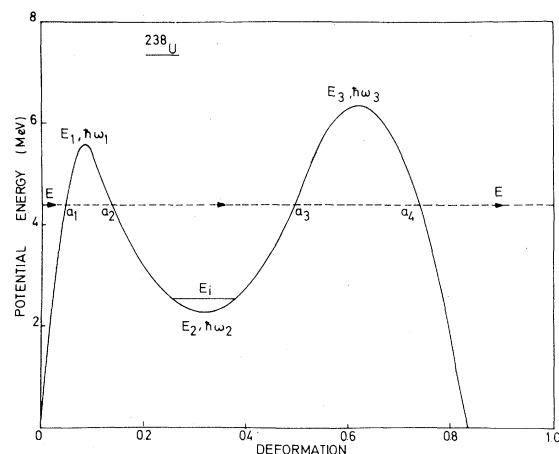


FIG. 2. Two-hump fission barrier in ^{238}U . The solid horizontal line in the second well corresponds to the shape-isomeric state (E_i). Other symbols are described in the text. The barrier parameters are $E_1=5.60$ MeV, $\hbar\omega_1=1.77$ MeV, $E_2=2.30$ MeV, $\hbar\omega_2=0.52$ MeV, $E_3=6.35$ MeV, $\hbar\omega_3=0.74$ MeV.

parabolas and is given by

$$V(\epsilon) = E_j \pm \frac{1}{2} \mu \omega_j^2 (\epsilon - \epsilon_j)^2, \quad (1)$$

where the plus sign applies for $j=2$ and the minus sign for $j=1$ and 3. E_j represent the maxima and minima of the potential, $\hbar\omega_j$ their respective curvature parameters, and ϵ_j the locations of the extrema on the deformation axis. $V(\epsilon)$ is taken to be zero at $\epsilon=0$. μ is the inertial mass parameter, assumed to be constant for all values of ϵ , and has the dimensions of the moment of inertia,²⁴ as ϵ , the distortion parameter, is dimensionless. The value of μ used in the calculation is

$$\mu = 0.054A^{5/3} \hbar^2 \text{ MeV}^{-1}. \quad (2)$$

The details of the penetrability calculation through two- and three-humped fission barriers in the WKB approximation have been reported by us earlier.^{25,26} Defining P_A , P_B , and P as the respective penetrabilities for the inner barrier alone, outer barrier alone, and the entire double-humped barrier, it has been shown^{27,28} that

$$P = P_A P_B / \{ [1 + ((1 - P_A)(1 - P_B))^{1/2}]^2 \cos^2 \nu_2 + [1 - ((1 - P_A)(1 - P_B))^{1/2}]^2 \sin^2 \nu_2 \}, \quad (3)$$

where the individual penetrabilities (P_A and P_B) in the WKB approximation are given²⁹ as

$$P_A = [1 + \exp(2\nu_1)]^{-1} \quad \text{and} \quad (4)$$

$$P_B = [1 + \exp(2\nu_3)]^{-1}$$

for energies below the top of the barriers, and

$$P_A = [1 + \exp(-2|\nu_1|)]^{-1} \quad \text{and} \quad (5)$$

$$P_B = [1 + \exp(-2|\nu_3|)]^{-1}$$

for energies above the top of the barriers. The quantities ν_j are the integrals in respective regions, as shown in Fig. 2, of the phase

$$K_1(\epsilon) = \{2\mu[E - V(\epsilon)]/\hbar^2\}^{1/2} = iK_2(\epsilon), \quad (6)$$

for example,

$$\nu_1 = \int_{a_1}^{a_2} K_2(\epsilon) d\epsilon, \quad \nu_2 = \int_{a_2}^{a_3} K_1(\epsilon) d\epsilon, \quad \nu_3 = \int_{a_3}^{a_4} K_2(\epsilon) d\epsilon. \quad (7)$$

The classical turning points a_1 , a_2 , a_3 , and a_4 are as shown in Fig. 2 for an excitation energy E .

The competition due to γ deexcitation to the isomeric state (which consequently fissions) has been simulated in the present work by including an absorptive (imaginary) part in the potential in the region of the second well. The calculation again uses the WKB approximation. Using the termin-

ology of Eqs. (3)–(7) with the added feature that the phase ν_2 now has added an imaginary part ($i\delta$), expressions for the prompt penetrability through the double barrier and for the absorption in the second well are found^{26,30} to be

$$P = (P_A P_B / \{e^{2\delta} + 2[(1 - P_A)(1 - P_B)]^{1/2} \cos 2\nu_2 + (1 - P_A)(1 - P_B)e^{-2\delta}\}) \quad (8)$$

and

$$L = P \left(\frac{e^{2\delta}}{P_B} - \frac{(1 - P_B)}{P_B} e^{-2\delta} - 1 \right), \quad (9)$$

respectively. For a complex potential ($V + iW$) in the region of the second well, the phase factor δ is given as

$$\delta = - \left(\frac{\mu}{2\hbar^2} \right)^{1/2} \int_{a_2}^{a_3} \frac{W(\epsilon)}{[E - V(\epsilon)]^{1/2}} d\epsilon, \quad (10)$$

provided

$$W(\epsilon) \ll [E - V(\epsilon)].$$

As expected, Eq. (8) reduces to Eq. (3), and L vanishes for $\delta=0$ ($W=0$). The flux absorbed in the second well is redistributed in different available channels and contributes a “delayed” fission penetrability term

$$P_D = L \left(\frac{P_B}{P_A + P_B + P_{\gamma_2}} + \frac{\kappa P_{\gamma_2}}{P_A + P_B + P_{\gamma_2}} \right), \quad (11)$$

where P_{γ_2} is the γ -deexcitation probability to the shape-isomeric state in the second well and κ is a fraction representing the average ratio of the probabilities of the spontaneous fission and the radiative decay to the first well for the isomeric state. We have accordingly chosen κ as²⁶

$$\kappa = \frac{\tau_i^\gamma}{\tau_i^f}, \quad (12)$$

where τ_i^γ and τ_i^f are the respective half-lives for the γ -decay and for the spontaneous fission of the shape-isomeric state and have been calculated for our static potential shape (Fig. 2) using the expressions given by Nix and Walker.³¹

As there is no time selection of the fission events in the subbarrier photofission measurements described earlier, the total fission penetrability (P') is the sum of the prompt fission penetrability (P) given by Eq. (8) and the delayed fission penetrability (P_D) given by Eq. (11):

$$P' = P + P_D. \quad (13)$$

The first term in the parentheses in Eq. (11) represents a fission contribution delayed by the time taken in the absorption and in the consequent redistribution of the flux in different available channels in the second well while the second term there

represents a contribution delayed further by the isomeric half-life. The remaining fraction of the absorption, which does not contribute to fission either directly or through the isomeric state, can be termed as "loss" and is given as

$$L' = L \left[1 - \left(\frac{P_B}{P_A + P_B + P_{\gamma_2}} + \frac{\kappa P_{\gamma_2}}{P_A + P_B + P_{\gamma_2}} \right) \right]. \quad (14)$$

The absorptive part, $W(\epsilon)$, of the potential in the second well has a parabolic shape with respect to the deformation parameter [similar to the real part $V(\epsilon)$] and increases linearly with the excitation energy. The functional form of $W(\epsilon)$ in the region of the second well used in this calculation is

$$W(\epsilon) = -W_0[E - V(\epsilon)], \quad (15)$$

where W_0 represents the strength of the damping and has been chosen to reproduce the width of the observed resonance structure in photofission cross section of ^{238}U near 5.7 MeV of photon energy as shown in Fig. 6 as well as the magnitude of the cross section on the shelf as shown in Fig. 5. The value used in this calculation is

$$W_0 = 3 \times 10^{-5}, \quad (16)$$

which is also consistent with the limits of the validity of Eq. (10). As this value of W_0 used in our calculation has been chosen by the requirement of reproducing satisfactorily the observed cross sections in a wide energy region, 2.5–6 MeV, it should, in turn, provide at least qualitatively reasonable estimates of the absorption and of the "loss" as defined in Eqs. (9) and (14), respectively, in this region of excitation.

B. Results

In Fig. 3 we have shown a sample calculation of the prompt and the total fission penetrability in ^{238}U . For energies greater than approximately 4.5 MeV, the dominant contribution to the fission yield is made by the prompt fission penetrability. However, below 4.5 MeV, the dominant contribution is made by the delayed fission penetrability and results in an isomeric shelf in the total penetrability as shown in Fig. 3. For excitations below the isomeric energy (2.56 MeV), the total penetrability is seen to fall very rapidly to coincide again with the prompt fission penetrability. The magnitude of the penetrability (cross sections) on the shelf is largely determined by the values of W_0 and that of the branching ratio κ and, therefore, defining κ in terms of Eq. (12) puts some constraints on the arbitrariness in the variation of the barrier parameters and leads to a somewhat self-consistent calculation of various observables such as fission half-lives and cross sections.

In Fig. 4 we have shown the behavior of the total

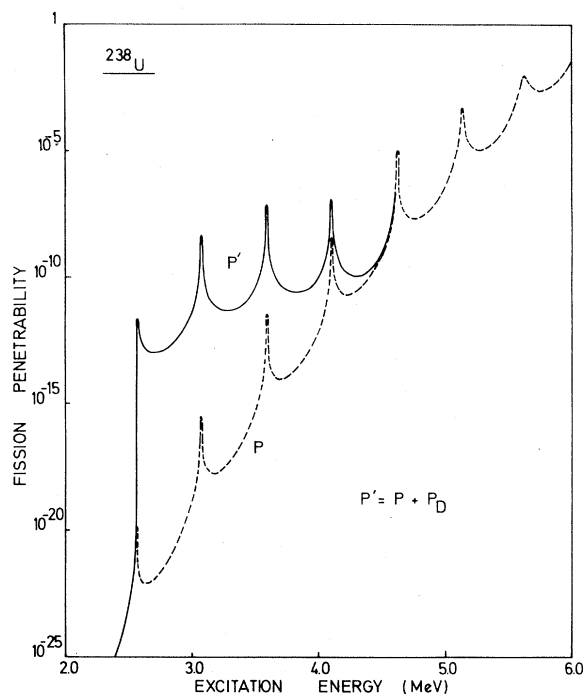


FIG. 3. Fission penetrability versus excitation energy for a two-hump fission barrier shown in Fig. 2. P , P_D , and P' represent, respectively, the prompt, the delayed, and the total fission penetrability.

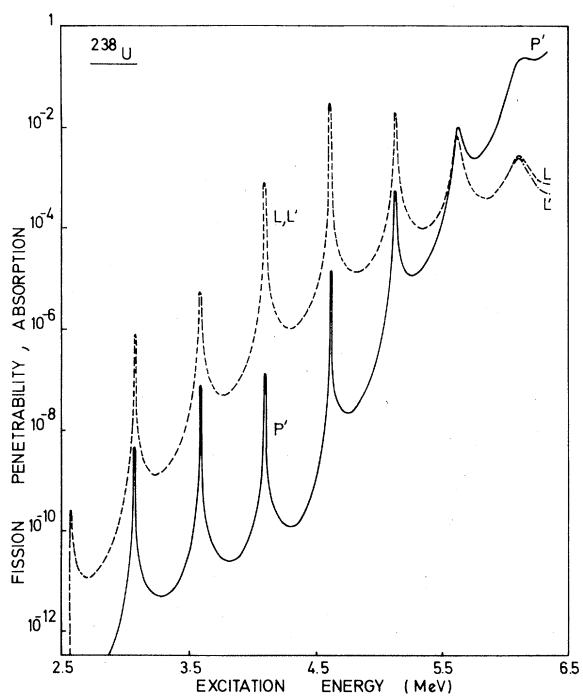


FIG. 4. Fission and absorption probabilities versus excitation energy for a two-hump fission barrier shown in Fig. 2. The symbols L , L' , and P' are defined in the text.

penetrability (P'), the absorption (L), and that of the loss (L') versus excitation energy in the sub-barrier photofission of ^{238}U . The fission contribution seems to be dominant above approximately 5.5 MeV. However, for excitations well below this energy only a negligible strength is seen in the fission channel. This explains the difficulties associated with fission cross-section measurements at energies well below the top of the barrier. L and L' seem to be essentially equal except for energies very close to the top of the barrier where P_B attains values comparable to unity.

IV. PHOTOFISSION CROSS-SECTION CALCULATION

The photofission cross section below the neutron threshold is related to the photoabsorption cross section by the expression

$$\sigma_{\gamma,f}(E_\gamma) = \sum_{J^\pi} \sum_K \sigma_{\gamma,\text{abs}}^{J^\pi} \frac{P_f^{J^\pi,K}}{P_f^{J^\pi,K} + P_{\gamma_1}^{J^\pi}}, \quad (17)$$

where J , π , and K represent, respectively, the total angular momentum, parity, and the component of J along the nuclear symmetry axis of the fissioning nucleus. $P_f^{J^\pi,K}$ represents the total fission penetrability in a given channel J^π, K . The total angular momentum J and the parity π are supposed to be conserved throughout the fission process. However, this is certainly not the case with K and, thus, at least in principle, quite different fission barriers are expected to be encountered in different J^π, K channels. A summation over all these individual channels is therefore needed to obtain the total photofission cross section. $\sigma_{\gamma,\text{abs}}^{J^\pi}$ and $P_{\gamma_1}^{J^\pi}$ are, respectively, the photoabsorption cross section and the radiative decay penetrability in the primary well in a given channel J^π . Thus, in order to calculate the photofission cross sections, one needs to know the photoabsorption cross section and the relative strength in the fission channel.

Reliable data on the cross section for dipole and quadrupole photoabsorption at low energies are not available. However, Axel³² has suggested the energy dependence of the total photonuclear dipole absorption cross section of heavy elements near 7 MeV excitation as

$$\sigma_{\gamma,\text{abs}}^{1-}(E_\gamma) = B \times (E_\gamma/7)^3 \times (0.01A)^{8/3} \text{ mb}. \quad (18)$$

With a normalization factor $B=3.5$, the magnitude of the cross section approximately fits^{20,33} the extrapolated giant-dipole resonance values in Ref. 18. This value of B is also consistent with the more recent observation by Zhuchko *et al.*²¹ that the original value of $B=5.2$ given by Axel³² leads to a substantial overestimation of the absorption cross section in the subbarrier energy region.

The suggested³² cross section below 3 MeV of photon energy is

$$\sigma_{\gamma,\text{abs}}^{1-}(E_\gamma) = 3.8 \times (E_\gamma/7)^2 \times (0.01A)^{7/3} \text{ mb}. \quad (19)$$

In Eqs. (18) and (19), E_γ is the photon energy in MeV and A is the mass number of the nucleus. The ratio of the quadrupole- to-dipole photoabsorption cross section is^{34,35} approximately equal to 0.02 for low energy γ rays of interest in this work. Therefore, one might expect the photoabsorption cross section to be given by the dipole absorption cross section in the absence of any significant enhancement of the quadrupole component in the energy region of our interest. The prediction³⁶ as well as the recent observation³⁷ of a giant electric quadrupole resonance in ^{238}U tend to locate it at an energy approximately equal to 9–10 MeV. This is well above the energy region of our interest in the present work. We have therefore used Eqs. (18) and (19) to represent the total absorption cross section.

The relative strength in the fission channel is determined in terms of the penetrabilities corresponding to fission and γ -deexcitation channels [Eq. (17)]. The fission penetrability is given by Eq. (13) and the radiative decay penetrabilities (P_{γ_1} and P_{γ_2}) have been calculated using a semi-empirical expression given by Bowman²²:

$$P_\gamma = 2\pi \times 4.1 \times 10^{-7} \times \exp(1.6E_\gamma). \quad (20)$$

This expression gives a radiative penetrability consistent with the dipole radiative transmission coefficient calculated in Ref. 38. We have therefore restricted ourselves only to the dipole channel corresponding to $J^\pi=1^-$ in the present calculation and have also not included the competition between $K=0$ and $K=1$ channels for the simple reason that most of this calculation is in the deep-subbarrier energy region where only the lowest barrier corresponding to $K=0$ will be most significant. This has been shown in Ref. 17, where the fission transmission coefficient in ^{238}U corresponding to $K=1$ channel is approximately one to two orders of magnitude smaller than that for $K=0$ channel in the threshold energy region. More recent analyses^{20,39} have also located the $K=1$ threshold approximately 500–600 keV above that corresponding to $K=0$. Thus, in the absence of any strong resonances in $K=1$ channel occurring at energies corresponding precisely to the minima in $K=0$ channel, a rather unlikely possibility, our assumption of neglecting the $K=1$ competition is reasonably justified.

V. RESULTS AND DISCUSSION

Using a suitable two-hump fission barrier (Fig. 2) in ^{238}U , we have calculated the subbarrier photo-

fission cross sections and the fission half-lives. In Fig. 5 we have shown a comparison of our calculated cross sections with those measured by Bowman *et al.*⁶ and by Zhuchko *et al.*^{8,10,21} The differences in the slopes of the cross sections in the isomeric-shelf region observed in these two measurements are significantly large and have been explained¹⁰ in terms of the large differences in the energy resolutions achieved in these two studies.

The solid line in Fig. 5 represents our results, calculated in steps of 10 keV each, showing a number of resonances in the subbarrier photofission cross sections. The crosses are the results of Bowman *et al.*⁶ using bremsstrahlung beam from a linear accelerator for photoexcitation. These cross sections were measured only at a few excitation energies, with an energy interval of 500 keV each, and with a relatively poor energy resolution. The filled circles represent the results of Zhuchko *et al.*^{8,10,21} again using the bremsstrahlung beam, but from a high-current microtron and claim a better resolution. The cross sections have also

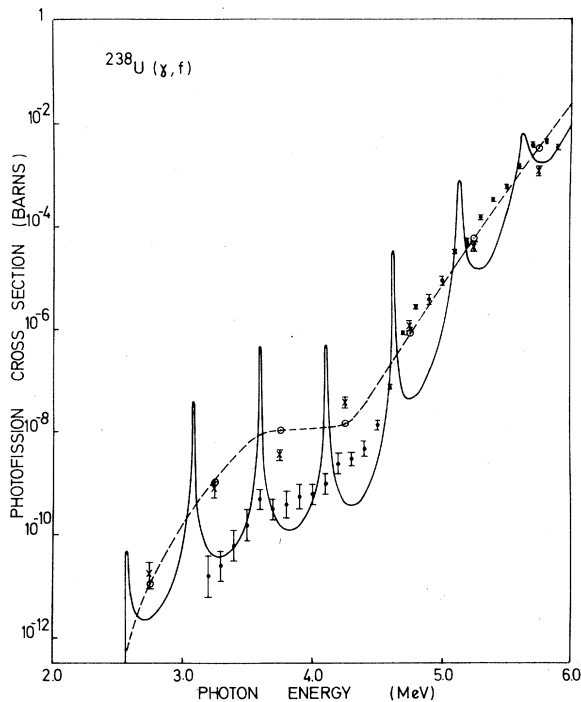


FIG. 5. A comparison of the calculated (solid line) subbarrier photofission cross section of ^{238}U with those measured by Zhuchko *et al.* (Refs. 8, 10, and 21) (filled circles). The open circles represent an average on our calculated cross sections over an energy interval of 500 keV for comparison with poor resolution data of Bowman *et al.* (Ref. 6) (crosses). The dashed line has been drawn through the open circles just to guide the eye and does not represent a "moving-average" on our calculated cross sections.

been measured more systematically with energy intervals of 100 keV each. These results show reasonable agreement with our calculation in the region of the isomeric shelf. In order to compare our results with those of Bowman *et al.*,⁶ we have calculated an average on our calculated cross sections over an energy interval of 500 keV at only those energies where the measured cross sections are given. These average cross sections are shown by the open circles and a dashed line has been drawn through these points just to guide the eye. This dashed line does not represent a "moving average" on our calculated cross sections. In view of the sharp resonance structures in our calculated cross sections, the shape of any such "moving average" shall depend crucially upon the choice of the averaging energy interval. For example, an average over the 200–300 keV interval shall still show resonance structures, though relatively much wider, in the cross sections, while an averaging interval much larger than 500 keV shall tend to distort the shape of the calculated curve which shows sharp resonances separated by approximately 500 keV each. We believe that these resonances should be readily observable on top of the isomeric shelf. This is because when the excitation energy is appropriate for the transmission resonance, there is a large amplitude for the wave function in the second well which augments both fission and γ -decay equally. Thus the fission output, whether prompt or delayed, is amplified at the resonance energy.

Figure 6 shows a comparison of our calculated results, averaged over the 100 keV energy interval, with those measured by Dickey and Axel¹⁷ using "tagged" bremsstrahlung with variable energy

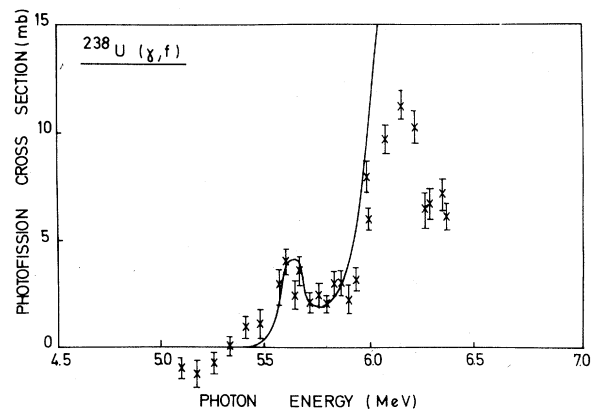


FIG. 6. A comparison of our calculated photofission cross sections (solid line) in the threshold region, averaged over an energy interval of 100 keV, with measured data of Dickey and Axel (Ref. 17) (crosses) using "tagged bremsstrahlung" with variable energy photons defined to 100 keV.

photons defined to 100 keV. The threshold resonance at 5.7 MeV is satisfactorily reproduced. The calculated cross section continues to rise above 6 MeV of photon energy. This is expected because we have not included the neutron competition in our calculation. The neutron threshold in ^{238}U is approximately 6.2 MeV and seems to be responsible for the observed decrease in photofission cross sections near this energy.

We have also calculated the ground state spontaneous fission half-life and the isomeric half-life using the two-hump fission barrier (Fig. 2) in ^{238}U . These estimates for the fission half-lives are, however, only of qualitative value as these have been calculated using a static potential shape with a constant mass parameter. It has been shown by Pauli and Ledergerber⁴⁰ that significantly different results could be obtained when dynamical effects are taken into account. Assuming a curvature ($\hbar\omega$) of 1.0 MeV for the primary potential well the value obtained for the ground state spontaneous fission half-life corresponding to the two-hump barrier of Fig. 2 in our calculation is equal to 1.167×10^{16} yr. This is in excellent agreement with the most recent measurement⁴¹ of this half-life yielding the value $(1.01 \pm 0.03) \times 10^{16}$ yr.

Similarly, for the isomeric state, assumed to be the ground state in the second well of the two-hump fission barrier shown in Fig. 2, we obtain the following results in our calculation for the isomeric-excitation energy and for the different components of the isomeric half-life:

$$\begin{aligned} E_i &= 2.56 \text{ MeV}, \\ \tau_i^{\gamma} &= 201 \times 10^{-9} \text{ sec}, \\ \tau_i^{\text{sf}} &= 220 \times 10^{-7} \text{ sec}, \\ \tau_i^{\text{total}} &= 199 \times 10^{-9} \text{ sec}. \end{aligned}$$

The isomeric excitation energy and the isomeric half-life are again in excellent agreement with those measured as 2.56 MeV⁴² and as $(195 \pm 30) \times 10^{-9}$ sec,⁴³ respectively. The two different components of the isomeric half-life yield a value for the fraction κ [Eq. (12)] equal to 0.913×10^{-2} in our calculation. This is also in good agreement with values obtained for this branching ratio as equal to 2×10^{-2} in Ref. 42 and equal to 1×10^{-2} in a more recent work.¹²

We would also like to comment here on a recent observation by Zhuchko *et al.* in Ref. 8 where they found that although the shelf in the photofission yield (cross sections) was evident only for photon energies below 4.5 MeV, an increase in the isotropic component of the fission fragment angular distribution was observed in the energy region 4.5–5.5 MeV. This led them to propose a “normal

isomeric shelf” in the energy region 4.5–5.5 MeV and an “anomalous shelf” in the energy region below 4.5 MeV. In the first proposed explanation of the occurrence of an isomeric shelf in the framework of a double-humped fission barrier, Bowman^{6,22} calculated only the average cross sections and thus neglected the effects of subbarrier resonances expected in such a model. However, with more refined measurements, Zhuchko *et al.*⁸ seem to have also observed the presence of such resonance structures in deep-subbarrier photofission cross sections. In the present work, we have included such resonance structures and believe that a further classification of the isomeric shelf into a “normal” and an “anomalous” one is unwarranted as both these belong to the same physical phenomenon and arise due to a nonvanishing delayed-fission contribution at higher energies. This is illustrated in Fig. 7 where we have shown the prompt- and the delayed-fission penetrabilities as a function of photon energy. The delayed-fission penetrability is dominant at energies below 4.4 MeV and results in a shelf in the measured photofission yields (cross sections). The two penetrabilities seem to be equal to each other at 4.4 MeV, above which the prompt penetrability begins to dominate. However, the delayed contribution does not vanish. In the energy region 4.4–5.2 MeV,

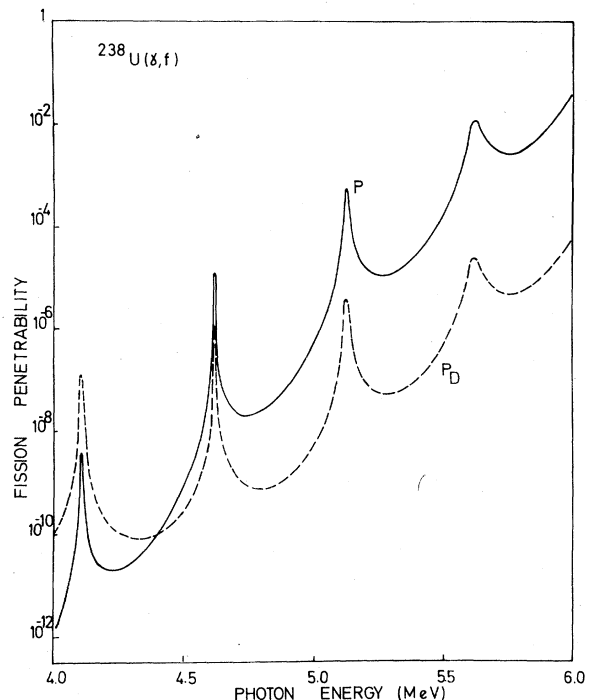


FIG. 7. Relative contributions of the prompt and the delayed fission probabilities in the photon energy region 4–6 MeV in the subbarrier photofission of ^{238}U .

the delayed contribution is about an order of magnitude smaller than that of the prompt penetrability. Such a small contribution may be difficult to be detected in a cross-section measurement. However, as the delayed-fission contribution is expected to result in a distinctly different (isotropic) angular distribution, an angular anisotropy measurement might be more sensitive to it. In a qualitative sense this seems to be exactly what has been observed recently in Ref. 8.

The parabolic shapes used in parametrizing the double-hump fission barrier in the present work are only an approximation. In reality the potential shapes could be quite different. However, our results indicate that such shapes are reasonably consistent with the observed fission characteristics of ^{238}U in the subbarrier energy region. Some of the discrepancies in the calculated cross sections versus those observed might be related to the lack of flexibility of the parabolic potentials used. The barrier parameters obtained in this work (Fig. 2) are consistent with those available in the literature^{20,44} except that we need a much narrower and thus a more penetrable inner barrier. Such features for the inner barrier have also been obtained recently by Bowman^{6,22} from the observed slope of the cross section in the shelf region and were claimed⁸ to be in contradiction with the inner barrier shapes obtained through an analysis of threshold photofission data. The present work shows that such a shape (Fig. 2) is reasonably consistent with cross sections in the entire subbarrier energy region, 2.5–6 MeV, and also reproduces reasonably correct fission half-lives.

The discrepancy in the peak value of the cross section in the resonance region on the isomeric shelf, for example near 3.6 MeV in Fig. 5, is, in our opinion, due to the difficulties associated with the energy resolution in the bremsstrahlung measurements. Although it is possible to reduce the peak value of the resonance to that observed^{8,10} by increasing the damping strength [Eq. (16)] used in our calculation, it would then be impossible to obtain an agreement with cross sections measured by Bowman *et al.*⁶ with a still poorer energy resolution. Furthermore, such a large damping shall result in the threshold resonance at 5.7 MeV (Fig. 6) to be much broader than that observed. These arguments are, of course, valid only if the observed cross sections in the entire subbarrier energy region correspond to a single fission path as assumed in the present work. Recent analyses⁴⁵ of fission probabilities for ^{238}U have suggested the possibility of two distinct second saddle points providing two independent paths to fission. However, even this analysis⁴⁵ concludes that for excitations below 6.5 MeV, fission is dominated

by the lower of the two outer saddle points thus justifying our assumption of a single fission path in the subbarrier energy region.

Finally there is some evidence for an apparent increase in the quadrupole component of the photofission angular distribution data¹³ below 6 MeV consistent with the more recent finding³⁹ of the apparent location of the $(J^\pi, K) = (2^+, 0)$ threshold at 5.5 MeV. This is approximately 500 keV below the $(1^-, 0)$ threshold³⁹ and results⁴⁶ in an inner barrier lowered by this much energy in $(2^+, 0)$ channel as compared to that in $(1^-, 0)$ channel. The outer barrier is, however, expected⁴⁶ to be equally high in both these channels. It is then important to inquire if such a lowering of the inner barrier could increase the quadrupole barrier penetrability to an extent that it may compensate for the otherwise low quadrupole photoabsorption probability. Such competition was first considered by Vandebosch⁴⁶ in an attempt to explain the dominance of the quadrupole component in near-threshold photofission of ^{240}Pu . It was, however, noted in our earlier work⁵ that, although such a competition was qualitatively consistent with the observations, it was not sufficient from a quantitative point of view. For ^{238}U , we have independently calculated the quadrupole-photofission cross section expected with the above mentioned modification in the double-hump barrier shape and found⁴⁷ that the quadrupole cross section is several orders of magnitude smaller than the dipole cross section in the isomeric-shelf region. However, in the threshold region the two differ only by an order of magnitude. An angular anisotropy measurement¹³ may perhaps be more sensitive to this small quadrupole contribution in the threshold region in the same way as discussed earlier in connection with the delayed-fission contribution in Fig. 7. We thus conclude that our neglecting the $(2^+, 0)$ channel in the present work does not affect the cross-section results in any significant way. Our conclusion is further confirmed by a more recent work⁴⁸ which attempted to analyze their isomeric-shelf data in ^{238}U in terms of a pure $(2^+, 0)$ channel and failed. This failure can be easily explained in our model calculation in terms of Eq. (12). A lowering of the inner barrier increases P_A , thus decreasing τ_i^γ and κ , which, in turn, leads to a significant decrease in the contribution of the delayed fission mainly responsible for the observed isomeric shelf.

ACKNOWLEDGMENTS

The author wishes to thank Professor D. S. Onley and Dr. D. Paya for valuable discussions,

and Dr. Yu. M. Tsipenyuk for sending cross-section data in tabular form. He also wishes to acknowledge the able assistance of Mr. F. Zamani-Noor in the early phase of this work. The author is also thankful to Dr. R. Joly, Dr. D. Paya, and

Dr. J. Blons for their hospitality during a year (1979–1980) spent at Centre d'Etudes Nucléaires de Saclay, France. The financial support for the visit was provided by the Commissariat à l'Énergie Atomique, France, and is gratefully acknowledged.

- ¹V. M. Strutinsky, Nucl. Phys. A95, 420 (1967).
- ²J. Blons, C. Mazur, D. Paya, M. Ribrag, and H. Weigmann, Phys. Rev. Lett. 41, 1289 (1978).
- ³A. Bohr, in *Proceedings of the International Conference on the Peaceful Uses of Atomic Energy, Geneva, Switzerland, 1955* (United Nations, New York, 1956), Vol. 2, p. 151.
- ⁴J. R. Huizenga, Nucl. Technol. 13, 20 (1972).
- ⁵B. S. Bhandari and I. C. Nascimento, Nucl. Sci. Eng. 60, 19 (1976).
- ⁶C. D. Bowman, I. G. Schröder, C. E. Dick, and H. E. Jackson, Phys. Rev. C 12, 863 (1975).
- ⁷V. E. Zhuchko, A. V. Ignatyuk, Yu. B. Ostapenko, G. N. Smirenkin, A. S. Soldatov, and Yu. M. Tsipenyuk, Zh. Eksp. Theor. Fiz. Pis'ma. Red. 22, 255 (1975). [JETP Lett. 22, 118 (1975)].
- ⁸V. E. Zhuchko, A. V. Ignatyuk, Yu. B. Ostapenko, G. N. Smirenkin, A. S. Soldatov, and Yu. M. Tsipenyuk, Phys. Lett. 68B, 323 (1977).
- ⁹C. D. Bowman, I. G. Schröder, K. C. Duvall, and C. E. Dick, Phys. Rev. C 17, 1086 (1978).
- ¹⁰V. E. Zhuchko, Yu. B. Ostapenko, G. N. Smirenkin, A. S. Soldatov, and Yu. M. Tsipenyuk, Yad. Fiz. 28, 1185 (1978) [Sov. J. Nucl. Phys. 28, 611 (1978)].
- ¹¹G. Bellia, L. Calabretta, A. Del Zoppo, G. Ingraio, E. Migneco, R. C. Barna, and D. De Pasquale, Lett. Nuovo Cimento 21, 373 (1978).
- ¹²G. Bellia, A. Del Zoppo, E. Migneco, R. C. Barna, and D. De Pasquale, Phys. Rev. C 20, 1059 (1979).
- ¹³N. S. Rabotnov, G. N. Smirenkin, A. S. Soldatov, L. N. Usachev, S. P. Kapitza, and Yu. M. Tsipenyuk, Yad. Fiz. 11, 508 (1970) [Sov. J. Nucl. Phys. 11, 285 (1970)].
- ¹⁴O. Y. Mafra, S. Kuniyoshi, and J. Goldemberg, Nucl. Phys. A186, 110 (1972).
- ¹⁵A. M. Khan and J. W. Knowles, Nucl. Phys. A179, 333 (1972).
- ¹⁶R. A. Anderl, M. V. Yester, and R. C. Morrison, Nucl. Phys. A212, 221 (1973).
- ¹⁷P. A. Dickey and P. Axel, Phys. Rev. Lett. 35, 501 (1975).
- ¹⁸A. Veyssière, H. Beil, R. Bergère, P. Carlos, A. Leprêtre, and K. Kernbath, Nucl. Phys. A199, 45 (1973).
- ¹⁹J. T. Caldwell, E. J. Dowdy, B. L. Berman, R. A. Alvarez, and P. Meyer, Los Alamos Scientific Laboratory Report LA-UR-76-1615 (unpublished); Phys. Rev. C 21, 1215 (1980).
- ²⁰L. J. Lindgren, A. Alm, and A. Sandell, Nucl. Phys. A298, 43 (1978).
- ²¹V. E. Zhuchko, Yu. B. Ostapenko, G. N. Smirenkin, A. S. Soldatov, and Yu. M. Tsipenyuk, Yad. Fiz. 28, 1170 (1978) [Sov. J. Nucl. Phys. 28, 602 (1978)].
- ²²C. D. Bowman, Phys. Rev. C 12, 856 (1975).
- ²³V. E. Zhuchko, A. V. Ignatyuk, Yu. B. Ostapenko, G. N. Smirenkin, A. S. Soldatov, and Yu. M. Tsipenyuk, Zh. Eksp. Theor. Fiz. Pis'ma. Red. 24, 309 (1976) [JETP Lett. 24, 277 (1976)].
- ²⁴J. D. Cramer and J. R. Nix, Phys. Rev. C 2, 1048 (1970).
- ²⁵B. S. Bhandari, Nucl. Phys. A256, 271 (1976).
- ²⁶B. S. Bhandari, Phys. Rev. C 19, 1820 (1979).
- ²⁷B. S. Bhandari, Ph. D. thesis, Ohio University, 1974 (unpublished).
- ²⁸T. Martinelli, E. Menapace, and A. Ventura, Lett. Nuovo Cimento 20, 267 (1977).
- ²⁹N. Fröman and P. O. Fröman, *JWKB Approximation* (North-Holland, Amsterdam, 1965), pp. 90–101.
- ³⁰B. S. Bhandari and D. S. Onley, IFUSP Report No. 87, São Paulo, Brazil, 1976 (unpublished).
- ³¹J. R. Nix and G. E. Walker, Nucl. Phys. A132, 60 (1969).
- ³²P. Axel, Phys. Rev. 126, 671 (1962).
- ³³L. J. Lindgren and A. Sandell, Z. Phys. A285, 415 (1978).
- ³⁴J. R. Huizenga and H. C. Britt, in *Proceedings of International Conference on Photoneuclear Reactions and Applications, Asilomar, California, 1973*, edited by B. L. Berman (Lawrence Livermore Laboratory, Livermore, California, 1973), p. 833.
- ³⁵J. M. Blatt and V. F. Weisskopf, *Theoretical Nuclear Physics* (Wiley, New York, 1952).
- ³⁶A. Bohr and B. R. Mottelson, *Nuclear Structure* (Benjamin, New York, 1975), Vol. II.
- ³⁷J. D. T. Arruda Neto, S. B. Herdade, B. S. Bhandari, and I. C. Nascimento, Phys. Rev. C 18, 863 (1978).
- ³⁸R. Vandenbosch and J. R. Huizenga, *Nuclear Fission* (Academic, New York, 1973).
- ³⁹J. D. T. Arruda Neto, S. B. Herdade, and I. C. Nascimento, Nucl. Phys. A334, 297 (1980).
- ⁴⁰H. C. Pauli and T. Ledergerber, in *Proceedings of the Third IAEA Symposium on the Physics and Chemistry of Fission, Rochester, 1973* (IAEA, Vienna, 1974), Vol. I, p. 463; also Nucl. Phys. A207, 1 (1973).
- ⁴¹R. L. Fleischer and P. B. Price, Phys. Rev. 133, B63 (1964).
- ⁴²P. A. Russo, J. Pedersen, and R. Vandenbosch, in *Proceedings of the Third IAEA Symposium on the Physics and Chemistry of Fission, Rochester, 1973* (IAEA, Vienna, 1974), Vol. I, p. 271; also Nucl. Phys. A240, 13 (1975).
- ⁴³K. L. Wolf, R. Vandenbosch, P. A. Russo, M. K. Mehta, and C. R. Rudy, Phys. Rev. C 1, 2096 (1970).
- ⁴⁴B. B. Back, O. Hansen, H. C. Britt, and J. D. Garrett, Phys. Rev. C 9, 1924 (1974).
- ⁴⁵A. Gavron, H. C. Britt, P. D. Goldstone, J. B. Wilhelmly, and S. E. Larsson, Phys. Rev. Lett. 38, 1457 (1977).

⁴⁶R. Vandenbosch, *Phys. Lett.* 45B, 207 (1973).

⁴⁷F. Zamani-Noor, M. S. thesis, Shiraz University, 1979 (unpublished).

⁴⁸R. Alba, G. Bellia, L. Calabretta, A. Del Zoppo,

E. Migneco, and G. Russo, in *Proceedings of the Fourth IAEA Symposium on the Physics and Chemistry of Fission, Jülich, 1979* (IAEA, Vienna, 1980).